Carbides and Carbon Control in MC – Reinforced Superalloys

Patrice Berthod[1*]

[1]*Department of Chemistry and Physics of Solids and Surfaces, IJL, University of Lorraine, P. O. Box 50840-54011, Nancy, France.*

Author's contribution

The sole author designed, analysed, interpreted and prepared the manuscript.

Original Research Article

ABSTRACT

Polycrystalline alloys based on cobalt and elaborated by classical foundry are known since the middle of the last century. They are currently still used, notably for geometrically complex components working at high temperature. Beyond the oldest ones reinforced by chromium carbides, new principles of carbides–strengthened cobalt–based alloys have recently appeared. MC–type refractory mono–carbides allow maintaining the melting start temperature at a high level when they are present as single carbide phase. Their high temperature stabilities and script–like morphologies also favor high mechanical properties at elevated temperatures. Optimized MC–carbides fractions can be obtained with carbon contents, close to 0.4 wt.%C, for achieving significant strengthening without threat for the low and high temperature toughness. Controlling the carbon content is thus of prior importance. Unfortunately the most common metallographic apparatus used for measuring the chemical composition of alloys – the Energy Dispersion Spectrometers (EDS) attached to Scanning Electrons Microscopes (SEM) – are not able to analyze, with sufficient accuracy, carbon with so low contents. A simple indirect method using both EDS and SEM is proposed here to get some information about the carbon content in several MC–reinforced Co–based superalloys.

Keywords: Carbides fractions assessment; carbon assessment; Superalloys; EDS; SEM.

_____

Corresponding author: E-mail: patrice.berthod@univ-lorraine.fr;

1. INTRODUCTION

Superalloys are metallic alloys presenting exceptional mechanical and chemical properties at high temperature. They are used for components working in the hottest parts of turbines and industrial processes. Most of them are based on iron (with significant presence of nickel), on nickel or on cobalt [1]. Many of the first superalloys to appear were {solid solution}–strengthened and carbides–reinforced [2]. Several decades ago, high performance superalloys emerged, such as the Oxide Dispersion Strengthened superalloys, the directionally–solidified alloys and the nickel–based single–crystals [3]. Such superalloys present particular microstructures which may be not adapted for geometrically complex components [4]. For such applications polycrystalline superalloys with an equi–axed structure can be more easily shaped, for instance by classical foundry. Their isotropic microstructure allows benefiting from a mechanical behavior which is homogeneous in all directions. However, in case of service intended at elevated temperature under significant applied stresses, the high densities of grain–grain and dendrite–dendrite interfaces require their reinforcement by refractory hard particles with well adapted morphologies. In this way eutectic carbides are ideal, thanks to both their interdendritic or intergranular locations and their imbrication with matrix. All carbides are not necessarily geometrically stable enough at very high temperatures. When exposed at 1000°C or more for several tens hours, chromium carbides – of the Cr_7C_3 stoichiometry for example – tend evolving from their initial acicular shape to become spheroids. This is less the case for most of MC carbides which are both highly refractory and resistant against geometric evolution. Furthermore, many MC carbides form at the expense of chromium carbides [5], even in alloys particularly rich in chromium to resist high temperature oxidation and corrosion [6–9]. It is therefore possible, by careful rating of the contents in carbon and in the strong MC-former metal, to achieve a dense interdendritic strengthening network of MC carbides exclusively. In classically cast {25–30wt.%Cr}–containing cobalt–based alloys, such interdendritic 100%MC networks made of TaC, HfC, NbC or ZrC were successfully obtained [10,11]. The same success was later encountered with TiC carbides [12,13]. Obtaining 100%MC–type superalloys closely depends on the contents in M and in C. Unfortunately the elaboration conditions possibly expose to the loss of the most oxidable elements because of the very high levels of the temperatures which must be reached (typically 1600–1700°C). In such conditions, even under "pure" argon, more or less significant losses may be possible during melting. M, generally strong carbide–former metal, is generally also very easy to nitride and to oxidize: thus significant masses of M can be lost as slag floating over the liquid metal. C can be easily oxidized as Co_x gases. It is therefore compulsory to well know the M and C contents really obtained in alloy. Wavelength Dispersion Spectrometry (WDS) (Castaing's microprobe, or available associated to some electron microscopes) or, more common, Energy Dispersion Spectrometry (EDS), often present attached to a Scanning Electron Microscope/SEM), are efficient analyzing means to specify the contents in all metallic elements including M. But they are not suitable for measuring the content in C because of the low molar mass of this light element and its very low content in carbides–reinforced superalloys (same contents as in a ferrite–pearlite steel). Only spark spectrometers and other less common apparatus are able to give C contents values accurate enough.

In this work, focus was done on five selected Cr–rich cobalt–based model superalloys. These ones involve three types of MC carbides, with M being a high atomic mass MC–former metal (tantalum), a low atomic mass MC–former one (titanium) and a medium atomic mass MC–former metal (zirconium). The chemical compositions of these five alloys were investigated simply using a scanning electron microscope (SEM) equipped with EDS and by exploiting the EDS spot analyses carried out on matrix. This allowed deducing the quantities of MC carbides and the minimal possible values of carbon content.

2. EXPERIMENTAL AND CALCULATION TECHNIQUES

The five cobalt–based alloys under interest in this study were earlier elaborated for testing new model superalloys: microstructure evolution during long exposure at high temperature, high temperature oxidation phenomena, creep behavior… There are:

- A TaC–containing one: Co(bal.)–25Cr–0.4C–6Ta (all contents in wt.%)

- Two TiC–containing ones: Co(bal.)–25Cr–0.25C–1Ti and Co(bal.)–25Cr–0.5C–2Ti (all contents in wt.%)
- Two ZrC–containing ones: Co(bal.)–25Cr–0.25C–1.9Zr and Co(bal.)–25Cr–0.5C–3.8Zr (all contents in wt.%)

Their chromium contents were rated at 25wt.%C for hot corrosion resistance purpose [6–9] and their carbon contents were chosen close to 0.4wt.% for a good compromise between the high temperature strength and a toughness high enough. The contents in MC–former elements were rated in order to obtain the same atomic contents as carbon, to promote the formation of MC as the single carbides present. All the alloys were synthesized by melting together millimetric parts of pure elements (purity >99.9%), by high frequency induction heating (CELES furnace, France) under a 300 millibars atmosphere of pure argon. The obtained ingots (about 40g each) were cut and samples were prepared for various thermal tests. One was embedded in an araldite resin (ESCIL, France), ground and polished until a mirror–like state was obtained. The five metallographic samples were observed by electron microscopy (SEM: JEOL JSM–6010LA, 20kV, Back Scattered Electrons/BSE mode), and chemically analyzed by Energy Dispersion Spectrometry/EDS to control the obtained chemical composition (except carbon) of the whole alloy (full frame analysis at ×250) and of the matrix (spot analysis).

The wished chemical compositions of the five alloys were well respected. The Ta, Ti or Zr contents in alloys were kept at the wished values (6 wt.% for Ta, 1 and 2 wt.% for Ti, 1.9 and 3.8 wt.% for Zr). The average values of the M content (M=Ta, Ti or Zr) in matrix obtained from a series of EDS spot analyses performed in the matrix of each alloy, were calculated. The results were used to determine, in a first time, the mass fractions of carbides, according to equation (1). In a second time, the volume fractions of carbides were calculated according to equation (2). To finish, the weight carbon content involved in the MC carbides were deduced according to equation (3).

$$f_{carb} = \frac{M_{carb}}{M_X - M_{carb} \times g_X^{mat}} \times \left(g_X^{all} - g_X^{mat} \right) \tag{1}$$

$$f_{carb}^{vol} = \frac{f_{carb} \ / \ \rho_{carb}}{(1 - f_{carb}) \ / \ \rho_{mat} \ + \ f_{carb} \ / \ \rho_{carb}} \tag{2}$$

$$g_C^{carb} = f_{carb} \times \frac{M_C}{M_{carb}} \tag{3}$$

Where:

g_X^{all} is the weight fraction of the carbide–former element X in the alloy

g_X^{mat} is the weight fraction of the carbide–former element X in the matrix

M_X is the molar mass of the carbide–former element X

M_C is the molar mass of carbon

M_{carb} is the molar mass of the carbide phase

f_{carb} is the mass fraction of the carbide phase

f_{carb}^{vol} is the volume fraction of the carbide phase

ρ_{mat} is the volume mass of the matrix

ρ_{carb} is the volume mass of the carbide

g_C^{carb} is the carbon weight content of alloy involved in MC carbides

3. RESULTS AND DISCUSSION

3.1 Chemical Compositions and Microstructures

The chemical compositions targeted for the five alloys, were well respected as previously demonstrated by full frame EDS control (except carbon). They are gathered in Table 1. Several SEM–BSE micrographs, illustrating the microstructures of these alloys, are available in Fig. 1 for the TaC–containing alloy, in Fig. 2 for the two TiC–containing alloys and in Fig. 3 for the two ZrC–containing alloys. The microstructure of the Co(bal.)–25Cr–0.4C–6Ta alloy (Fig. 1) is made of a dendritic matrix (Co–based solid solution of Cr, and possibly of Ta and C too, shown by the ǂ symbol), and of white TaC carbides (shown by the Ж symbol). These ones are interdendritic and closely imbricated with the periphery of the matrix dendrites. Their location and their script–like morphology indicate that they are certainly of a eutectic origin. The Co(bal.)–25Cr–0.25C–1Ti alloy (Fig. 2 top) is also made of a dendritic matrix (Co–based solid solution of Cr, and possibly of Ti and C too) and of carbides. These ones are mainly eutectic script–like black TiC carbides. The Co(bal.)–25Cr–0.50C–2Ti alloy (Fig. 2 bottom) is similar, but with a TiC network more developed.

Table 1. Chemical compositions of the five alloys

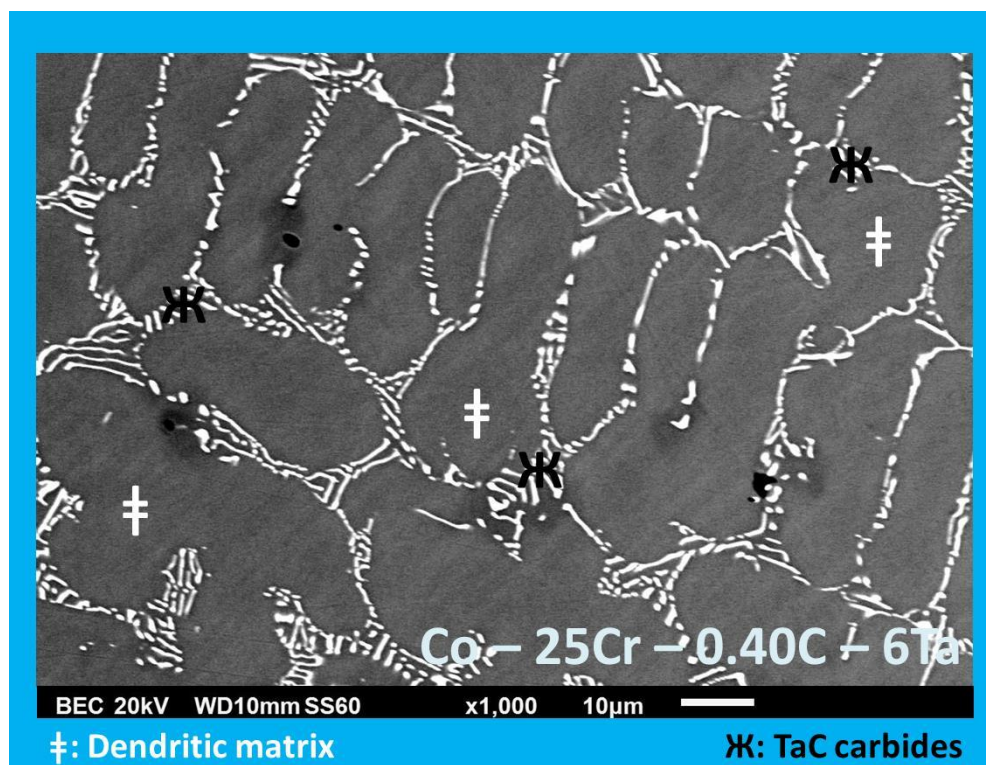| Co(bal.) – 25Cr – xC – yM (wt.%)				
M =	**Ta**	**Ti**		**Zr**
x (wt.%) =	0.4	0.25	0.50	0.25	0.50
y (wt.%) =	6	1	2	1.9	3.8

Fig. 1. SEM–BSE micrograph illustrating the microstructure of the TaC–containing alloy (Co(bal.)–25Cr–0.4C–6Ta, wt.%, C content targeted, not controlled)

The microstructures of the Co(bal.)–25Cr–0.25C–1.9Zr and Co(bal.)–25Cr–0.5C–3.8Zr alloys are shown in Fig. 3 (top and bottom respectively). They both contain a dendritic matrix and eutectic ZrC carbides. The ZrC / matrix boundaries are much fuzzier than the TaC / matrix and TiC / matrix in the three previous alloys. However, one can well distinguish the script–like shape of the ZrC carbide part of the interdendritic eutectic compound. The grey levels of the ZrC carbides and of matrix are almost similar. This is due to the proximity of the average molar mass of carbide and matrix which is much higher than for the TaC–containing alloy (average molar mass significantly higher for the white carbide than for the grey matrix) and for the TiC–containing ones (average molar mass significantly lower for the black carbide than for

the grey matrix). Some rare brighter particles are also present. This is not very possible to specify them, but one can guess that they are Zr_2C carbides (stoichiometry leading to an average molar mass really higher than for matrix). These other particles represent a very minor fraction and they will be not taken into account in the calculations.

3.2 EDS Measurement of the M Content in Matrix

A series of EDS spot measurements of the composition of matrix was carried out in the center of the dendrites arms. The average value of the content in the MC–former element was calculated. The obtained values are displayed in Table 2 in which the M contents in the whole

alloys are also reminded. It appears that a significant part of the M element is still present in the matrix of the TiC–containing alloys (between a quarter and a half) while it is almost absent in the matrix of the ZrC–containing alloys. The case of the TaC– containing alloy is similar to the one of the alloy with TiC carbides since a third of the whole tantalum is present in the matrix.
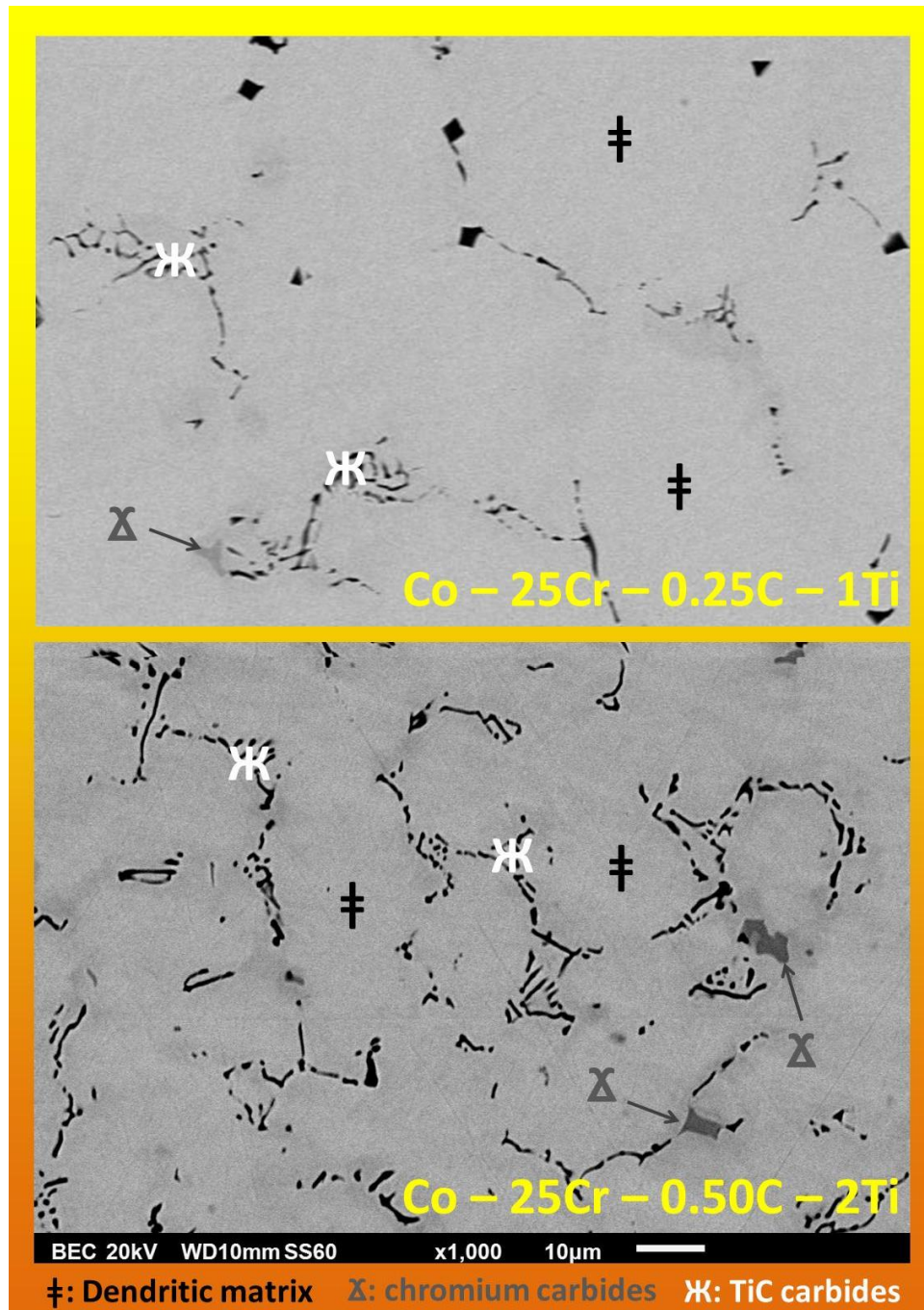

Fig. 2. SEM–BSE micrographs illustrating the microstructure of the two TiC–containing alloys (Co(bal.)–25Cr–0.25C–1Ti and Co(bal.)–25Cr–0.50C–2Ti, wt.%, C contents targeted, not controlled)
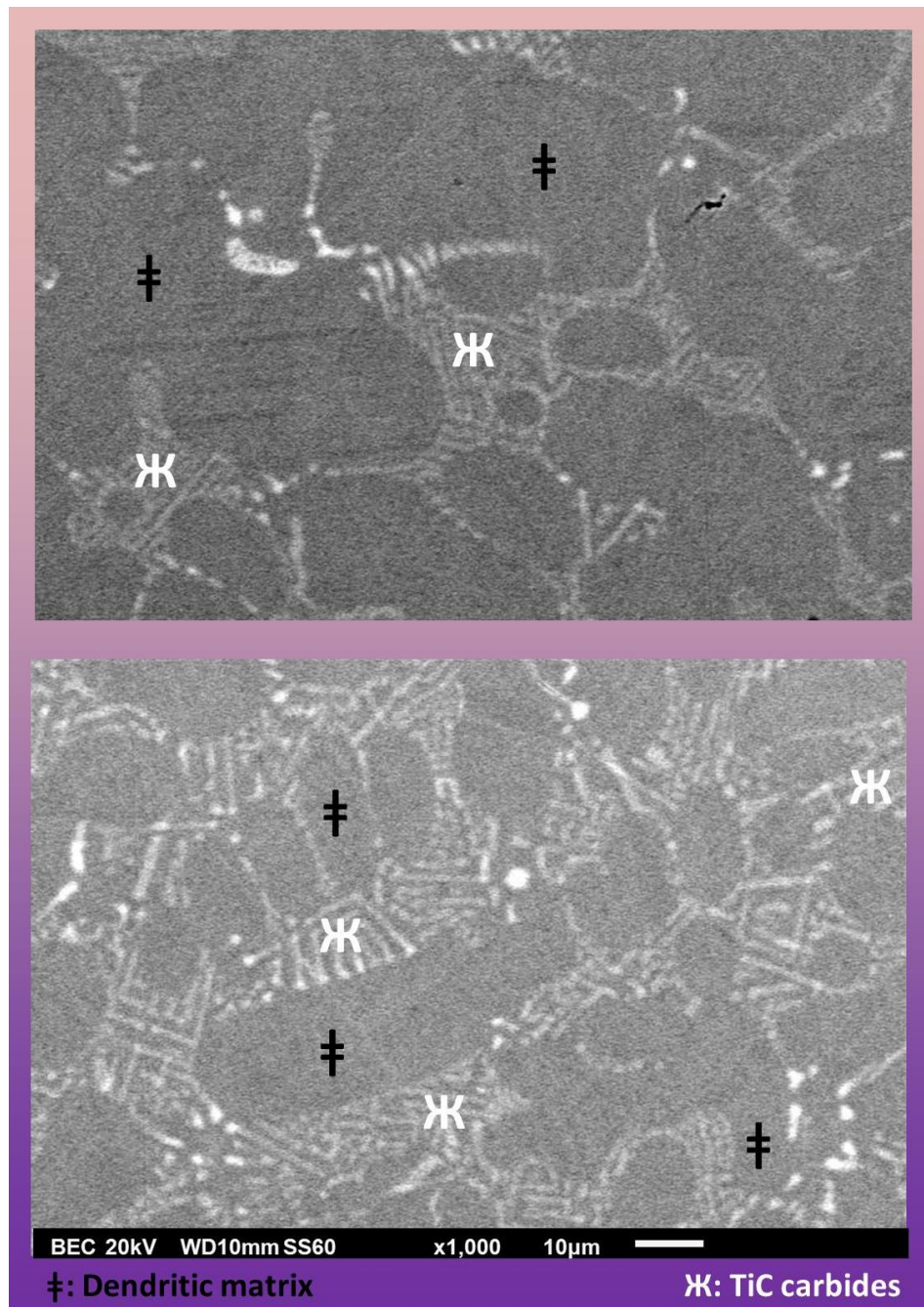
Fig. 3. SEM–BSE micrographs illustrating the microstructure of the two ZrC–containing alloys (Co(bal.)–25Cr–0.25C–1.9Zr and Co(bal.)–25Cr–0.50C–3.8Zr, wt.%, C contents targeted, not controlled)

3.3 Mass and Volume Fractions of Carbides and Repartition of C

The difference in M weight content between alloy and matrix will be exploited to deduce the values of the mass fractions of the MC carbides in each of the five alloys, according to equation (1). The corresponding volume fraction was calculated according to equation (2), and the part of the weight content in carbon of the alloy involved in

the carbides was deduced using equation (3). The results, obtained using the values of molar mass and volume mass listed in Table 3, are presented in Table 4 for the TaC–containing alloy, Table 5 for the two TiC–containing alloys and Table 6 for the two ZrC–containing alloys.

For the TaC–containing alloy, in which about 2.2 wt.%Ta out of the 6 wt.% present in alloy is not used to form carbides, the TaC mass fraction is almost 4.2% and the corresponding volume fraction is close to 2.7%, lower than the previous numerical value consequently to the high volume mass of the TaC phase (much higher than for matrix). Only two thirds of the carbon content is thus involved in the TaC carbides and the matrix ought to contain up to 0.14 wt.%. The real C content in matrix can be slightly or significantly lower than these 0.14 wt.%C because of possible carbon loss during the elaboration.

Table 2. Weight contents in MC–carbide former element in the whole alloys, and in their matrixes, as specified by EDS spot analysis

Co(bal.) – 25Cr – xC – yM (wt.%)					
M =	Ta	Ti		Zr	
X content	6	1	2	1.9	3.8
in alloy	wt.%	wt.%	wt.%	wt.%	wt.%
X content	2.19	0.29	0.83	0.04	0.14
in matrix	wt.%	wt.%	wt.%	wt.%	wt.%

Table 3. Reminder of the values of the molar masses of each M element, of the corresponding MC carbide, and of the volume masses of these MC carbides (an average volume mass of 9 g / cm^3 has been fixed for the matrixes of all alloys)

Co(bal.) – 25Cr – xC – yM (wt.%)					
M =	Ta	Ti		Zr	
M_X	180.95 g/mol	47.867 g/mol	47.867 g/mol	91.224 g/mol	91.224 g/mol
M_{carb}	192.96 g/mol	59.877 g/mol	59.877 g/mol	103.234 g/mol	103.234 g/mol
ρ_{mat}	9 g / cm^3	9 g / cm^3	9 g / cm^3	9 g / cm^3	9 g / cm^3
ρ_{carb}	14.3 g / cm^3	4.93 g / cm^3	4.93 g / cm^3	6.73 g / cm^3	6.73 g / cm^3

Table 4. Mass and volume fractions of TaC carbides; part of C involved in carbides and maximal C content in matrix

Co(bal.) – 25Cr – 0.4C – 6Ta (wt.%)				
Wt.% Ta in matrix	Mass.% of TaC	Vol.% of TaC	Wt.%C as TaC	Wt.%C in matrix
2.19	4.16	2.66	0.26	0.14 max

Table 5. Mass and volume fractions of TiC carbides; part of C involved in carbides and maximal C content in matrix

Co(bal.) – 25Cr – xC – yTi (wt.%)					
	Wt.% Ti in matrix	Mass.% of TiC	Vol.% of TiC	Wt.%C as TiC	Wt.%C in matrix
0.25C – 1Ti	0.29	0.89	1.61	0.18	0.07 max
0.50C – 2Ti	0.83	1.48	2.68	0.30	0.20 max

Table 6. Mass and volume fractions of ZrC carbides; part of C involved in carbides and maximal C content in matrix

Co(bal.) – 25Cr – xC – yZr (wt.%)					
	Wt.% Zr in matrix	Mass.% of ZrC	Vol.% of ZrC	Wt.%C as ZrC	Wt.%C in matrix
0.25C – 1.9Zr	0.04	2.11	2.80	0.25	*0*
0.50C – 3.8Zr	0.14	4.14	5.46	0.48	*0.02 max*

Similar comments may be done for the results concerning the TiC–containing alloys and the ZrC alloys, except for the volume fraction of TiC and of ZrC which are higher than the mass fractions because of the volume masses of these carbides which are lower than the matrix one.

3.4 Consequences for the Conditions of Image Analysis for MC Carbides

Knowing now the volume fractions of MC carbides, and assuming that volume fractions and surfaces fractions are equivalent in absence of any preferential microstructure orientation, it is possible to look for the rating in grey level which separate the pixels which are devoted to become black and the ones which are devoted to become white. This was tested only for the alloys with MC carbides in quantity high enough, as is to say the alloys with at least 0.4wt.%C: Co(bal.)–25Cr–0.4C–6Ta (Fig. 4), Co(bal.)–25Cr–0.5C–2Ti (Fig. 5) and Co(bal.)–25Cr–0.5C–3.8Zr (Fig. 6),

In the case of the TaC–containing alloy, reaching the 2.66 surf.% of carbides necessitates to rate the threshold at a value higher than expected. With this adjustment, the TaC become "emaciated" but they are still recognizable and their script–like morphology remains unaffected. However it is true that this is not the rating that one is tempted to adopt when one looks to the SEM–BSE micrograph. The fact that the TaC carbides occupy a greater surface fraction outwardly is probably due to the high average molar mass of the TaC phase compared to the matrix one (this is almost twice for the TaC carbides). Consequently, when the scanning electron beam comes near an emerging tantalum carbide, the interaction peer intersects a part of the carbide existing close to the mirror–like surface. Consequently, the back scattered electrons emitted by this not really emerging part of the TaC carbide are taken into account in the signal even if they do not come from a really emerging part of the tantalum carbide. The surface fraction of "emerging" carbide is thus overestimated.

This is different for the alloy with TiC carbides. These titanium carbides appear much darker than matrix (average atomic number globally twice lower than the matrix's one), the threshold rating to reach the surface fraction equivalent to the 2.68 vol.% TiC deduced from the Ti content in matrix leads to an image which really looks like the SEM–BSE one. Therefore, natural grey level rating may automatically lead to very correct surface fractions.

The case of the ZrC–containing alloy is particular. The ZrC carbides appear only a little brighter than matrix. If one calculates the average molar mass or the average atomic number one should find a value a little lower than the matrix's one, and not a little higher as suggested by the molar mass hierarchy. This slightly higher brightness of the ZrC carbides by comparison to the matrix may be due to a small deviation from the 1 – 1 stoichiometry between Zr and C. A little more Zr atoms in the carbide than C atoms may explains this inconsistency. The presence of rare particles really brighter than matrix may confirm this hypothesis since these rare bright particles are possibly Zr_2C carbides. In such case this should demonstrate that there are maybe no carbon atoms enough to form the ZrC carbides (with the 1 – 1 stoichiometry) with all the Zr atoms available in the alloy since no Zr is present in the matrix (Table 6). The ZrC carbides appeared as rather fuzzy, maybe because of the proximity of the grey levels between them and matrix. In contrast, with the TaC and TiC carbides which were well defined and thus easy to analyze for knowing their emerging surface fractions (however with overestimation in the TaC case), measuring the surface fractions of the emerging ZrC carbides is complex, even impossible. Deducing first their mass fractions from the Zr contents in matrix and in alloy, then their volume fraction, was thus particularly useful.

Concerning carbon, it is thus as inexistent in matrix as Zr. More precisely, both must be only almost inexistent; otherwise carbides must be not stable since activities must be close to one another in carbides and in matrix. This is different for the other carbides in which one noticed the presence of Ta or Ti in significant contents in the matrix. For these alloys a part of carbon probably stay in matrix with higher contents than for the alloys with ZrC carbides, but maybe not as high as the values presented in Table 4 and Table 5. One cannot affirm that no carbon was lost during elaboration but one can think that the carbon losses were, for all alloys, not important and maybe even, not significant.
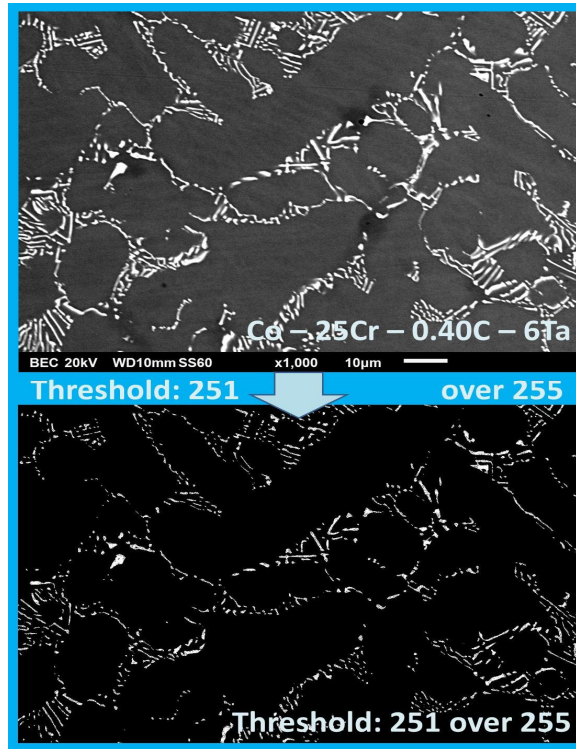
Fig. 4. SEM–BSE micrograph of the Co(bal.)–25Cr–0.4C–6Ta alloy and the best threshold rating which allows obtaining a surface fraction which is the closest to the 2.66 vol.% of TaC present in Table 4
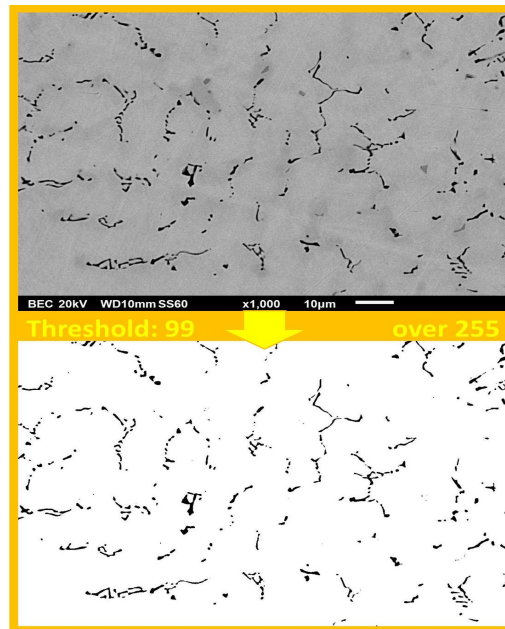

Fig. 5. SEM–BSE micrograph of the Co(bal.)–25Cr–0.5C–2Ti alloy and the best threshold rating which allows obtaining a surface fraction which is the closest to the 2.68 vol.% of TiC present in Table 5
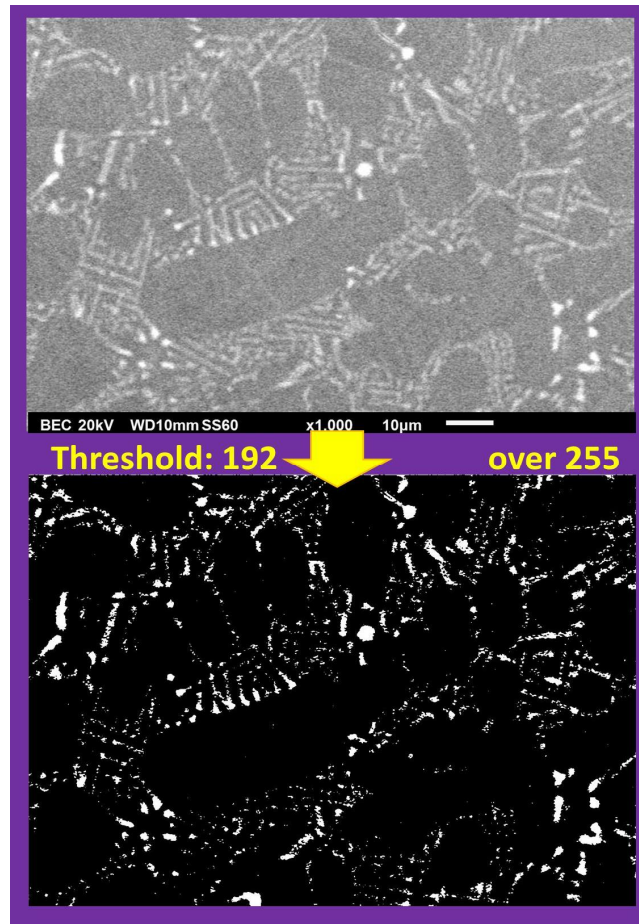
Fig. 6. SEM–BSE micrograph of the Co(bal.)–25Cr–0.5C–3.8Zr alloy and the best threshold rating which allows obtaining a surface fraction which is the closest to the 5.46 vol.% of ZrC present in Table 6

4. CONCLUSION

Carbon is an important element for all the superalloys, the strengthening of which is based on the presence of primary (and also secondary) carbides. Introducing this light element in the chemical composition of alloys elaborated by casting, for instance as graphite in the charge to melt, must be done carefully to efficiently trap it by the forming liquid metal. The atmosphere must be inert enough to avoid carbon oxidation and its loss as gaseous species. In absence of chemical composition analyzers able to specify low contents in carbon, the metallographic characterization of produced alloy may give useful estimation of the carbon content really obtained in the alloy. Obviously, simply analyzing the residual carbide–former metal in the alloy's matrix gives important information, with probably a better reliability than surface fraction measurements of carbides for which deviations may occur, as encountered here with TaC particularly.

COMPETING INTERESTS

The author has declared that no competing interests exist.

REFERENCES

1. Bradley E. Superalloys: A Technical Guide. Metals Park, USA: ASM International; 1988.
2. Sims CT, Hagel WC. The Superalloys. New York, USA: John Wiley & Sons; 1972.
3. Donachie MJ, Dobachie SJ. Superalloys: A Technical Guide (2nd ed.). Materials Park, USA: ASM International; 2002.

4. Durand-Charre M. The Microstructures of Superalloys. Boca Raton, USA: CRC Press; 1997.

5. Shatynski SR The thermochemistry of transition metal carbides. Oxid Met. 1979;13(2):105–118.

6. Kofstad P. High Temperature Corrosion. London, UK: Elsevier applied science; 1988.

7. Young DJ. High Temperature Oxidation and Corrosion of Metals. Amsterdam, The Netherlands: Elsevier corrosion series; 2008.

8. Di Martino J, Rapin C, Berthod P, Podor R, Steinmetz P. Corrosion of metals and alloys in molten glasses. Part 1: glass electrochemical properties and pure metal (Fe, Co, Ni, Cr) behaviours. Corr Sci. 2004;46:1849–1864.

9. Di Martino J, Rapin C, Berthod P, Podor R, Steinmetz P. Corrosion of metals and alloys in molten glasses. Part 2: nickel and cobalt high chromium superalloys behaviour and protection. Corr Sci. 2004;46:1865–1881.

10. Berthod P. Microstructure and hardness of several chromium-containing Co-based alloys reinforced by MC (TaC, NbC or HfC) carbides in as-cast or heat-treated conditions. Mater Sci Ind J. 2008;4(4): 290–296.

11. Berthod P. High temperature properties of several chromium-containing Co-based alloys High temperature properties of several chromium-containing Co-based alloys reinforced by different types of MC carbides (M= Ta, Nb, Hf and/or Zr). J Alloys Compd. 2009;481:746–754.

12. Khair M, Berthod P. As–cast microstructures and hardness of chromium–rich cobalt–based alloys reinforced by titanium carbides. Mater Sci Ind J. 2016;14(13):102–109.

13. Berthod P, Khair M. Thermodynamic and experimental study of cobalt-based alloys designed to contain TiC carbides. Calphad. 2019;65:34–41.

Peer-review history:
The peer review history for this paper can be accessed here:
http://www.sdiarticle4.com/review-history/58048